PADEU | PADEU **17**, 135 (2006)
ISBN 963 463 557, ISSN 0238-2423

An asteroid model of the mid- and far-infrared sky

Cs. Kiss[1], A. Pál[2], Th. Müller[3], P. Ábrahám[1]

[1]Konkoly Observatory, PO Box 67, H-1525 Budapest, Hungary
[2]Eötvös University, Department of Astronomy, H-1518 Budapest, Pf. 32, Hungary
[3]Max-Planck-Institut für extraterrestrische Physik, Giessenbachstrasse, D-85748 Garching, Germany

E-mail: pkisscs@konkoly.hu

Abstract
We developed a statistical model for the asteroid component of the far-infrared sky for wavelengths $5\,\mu\mathrm{m} \leq \lambda \leq 1000\,\mu\mathrm{m}$ based on the Statistical Asteroid Model (Tedesco et al., 2005). Far-infrared fluxes of ∼1.9 million asteroids are used to calculate confusion noise values and expected asteroid counts for space IR instruments in operation or in the near future. Our results show that the confusion noise due to asteroids will not increase the detection threshold for most of the sky. However, there are specific areas near the ecliptic plane where the effect of asteroids can be comparable to the contribution of Galactic cirrus emission and of the extragalactic background.
Keywords: *Infrared: Solar System, Asteroids*

1 Introduction

Currently, 329 777 minor planets are known[1] (as of March 16, 2006) in our Solar System, of which about 99% are located in the main belt. On the plane of the sky the vast majority of main-belt asteroids (MBA) are found at ecliptic latitudes beween ±20°. Their sizes range from a few ten meters up to about 1000 km. With temperatures between 200 and 300 K, the asteroids emit predominantly at thermal wavelengths between 5 μm and the millimetre range.

[1]http://cfa-www.harvard.edu/iau/lists/ArchiveStatistics.html

Deep infrared observations close to the ecliptic will therefore always include some of these moving targets (e.g. Tedesco & Désert 2002; Meadows et al. 2004). Such observations also show that only a small fraction of the existing minor body population is currently known and that this population might cause a non-negligible confusion noise contribution at certain wavelengths for specific instruments.

Recently several authors calculated confusion noise and detection limits for current/future infrared (IR) space missions (Spitzer, Akari, Herschel and SPICA). These papers focus on the two major confusion noise components: the extragalactic background (e.g. Negrello et al., 2004), the Galactic cirrus emission (Kiss et al., 2005; Jeong et al., 2005), or the combination of the two (Jeong et al., 2006).

It is an important question whether faint asteroids, which are individually below the detection limits, could contribute significantly to the confusion noise of these instruments. In order to take into accound these asteroids, a reliable statistical model is needed, which also includes minor bodies smaller than a few kilometers in diameter. Recently, Tedesco et al. (2005) presented the "Statistical Asteroid Model" (hereafter SAM). This model is based on a population of $\sim 1.9 \times 10^6$ asteroids obtained from the complete known asteroid sample (as of 1999), plus extrapolation of the size-frequency distribution (SFD) of 15 asteroid dynamical families and three background populations, to a diameter limit of 1 km. The main belt asteroid SFD can be described by a power law where the cumulative number of asteroids smaller than a given size $N(> D)$ is proportional to $D^{-\gamma}$. The SAM uses a value of $\gamma \simeq 2.8$ down to $\mathrm{D} \approx 1\,\mathrm{km}$. The validity of the SAM was demonstrated by comparing SAM predictions with ISO measurements at 12 μm (Tedesco and Desert, 2002) and Spitzer measurements at the 8 and 24 μm bands (Meadows et al., 2004). Asteroid counts from both surveys show good agreement with the SAM predictions.

For our calculations we used the *Statistical Asteroid Module* file from the SAM database[2], containing orbital elements, absolute magnitudes (H_{mag}), diameters and albedos for 1 880 987 objects. The tabulated values form the basis to calculate i) the position of each asteroid in the sky for a given epoch ii) the brightness of each asteroid at any given wavelength. For practical purposes we limited the position calculations to the time period between July 1, 1999 and June 30^{th} 2000, and the wavelength range from 5 μm (where the thermal emission starts to dominate the spectral energy distribution) to about 1 mm (to cover future far-IR/sub-mm space instruments).

[2] http://www.psi.edu/pds/SAM-I/

2 Data processing

Position calculation: Orbital elements of all SAM asteroids, including real and artifical ones were calculated for different epochs between the time span July 1999 and June 2000 with the average step size of 5 days. This step size is sufficient for yielding a good solar elongation coverage during one year. The orbital elements were obtained using accurate numerical integrations including the effect of all inner and outer planets (except for Pluto). From the orbital parameters the apparent ecliptical coordinates, distances and magnitudes were derived using the spatial coordinates of the Earth itself and the absolute magnitudes (which are known from the SAM database). The difference between the spatial position of the barycenter of the Earth-Moon system and the prospective position of the satellites is negligable for the apparent distribution of the asteroids.

Thermal brightness calculation: For the brightness calculations we applied the Standard Thermal Model (STM; Lebofsky et al. 1986). This model uses the true observing geometry for a given epoch, based on the heliocentric and geocentric distances and the phase angle. The asteroids are described as smooth, spherical and non-rotating bodies in instantaneous equilibrium with the solar radiation, no heat conduction into the surface is considered. The correction for beaming, shape and conductivity effects is done via the η-parameter with a value of $\eta = 0.756$. Furthermore, the flux at non-zero solar phase angles is obtained by applying an empirical phase correction of 0.01 mag/deg to the flux calculated at opposition. The STM has clear limitations with respect to flux accuracy (e.g., Müller & Blommaert 2004) or for modelling of minor bodies outside the main-belt (e.g., Harris 1998), but highly accurate flux predictions are not mandatory for our project. The STM predictions fulfill our needs to estimate fluxes for all objects in the specified time period and wavelength range.

Confusion noise calculation: A grid of $0.5' \times 0.5'$ cells was defined in the sky (in ecliptic coordinates). We determined the asteroid counts above specific flux limits for each cell, as well as the confusion noise due to asteroids in that particular cell. The confusion noise was calculated from the 'observed' distribution of all asteroids in that specific cell for each wavelength λ_i:

$$\sigma_a(\lambda_i)^2 = \left(\frac{\Omega_c}{\Omega_p}\right) \sum_j S_j^2(\lambda_i) \qquad (1)$$

where Ω_c and Ω_p are the effective solid angle of the counting cell and the pixel of the observer instrument, respectively, and S_j is the observed flux of the asteroid

at λ_i. Note, that Ω_p is not necessarily the geometrical size of an instrument pixel but is modified by the properties of the optical system (like beam size). The sum runs over all asteroids in a counting cell.

These σ_a confusion noise values are *lower limits*, since there is an unknown contribtuion of small (fainter) asteroids, which is not considered here. However, bright asteroids are the dominant sources of confusion and asteroids smaller than $\sim$1 km in diameter would not contribute to the confusion noise significantly. We also note, that this confusion noise value is *per pixel* confusion noise. The confusion noise applicable for e.g. detection limits of point sources depends on the method used to extract/reconstruct the point source flux.

3 Results

Using these model calculations we have constructed all-sky confusion noise maps and calculated expected number counts for the sensitivity limits of several IR instruments. These results can be found under the URL: *"http://kisag.konkoly.hu/confnoise"*.

Our general results are summarized as follows: (I) The main trend shows a strong concentration of asteroids and a corresponding peak of confusion noise at the local anti-solar point and an extended "cloud" is present around the current maximum (see the example in Fig. 1). Seasonal variations are also not negligible. (II) Survey instruments working in the mid-infrared domain (like Spitzer/MIPS at 24 μm and Akari/IRC) may be strongly affected by confusion noise in the vicinity of the ecliptic plane. Such surveys should have already detected many faint asteroids serendipitously. (III) For 3 m-class IR telescopes, like Herschel or SPICA, asteroid confusion would not be negligible in anti-solar direction, however, solar aspect constraints for satellites usually do not allow to observe towards opposition targets.

4 Limitations of the model

The SAM is limited to asteroids with a lower limit in size of $\sim$1 km in diameter, but there is a population of asteroids with sizes below this limit. As can be verified with Eq. 1, the impact of very small bodies (a few hundred meters in diameter and below) is minor to the confusion noise.

In our model we considered only asteroid families covered in the SAM, i.e. most of our asteroids are MBAs, with typical temperatures in the order of

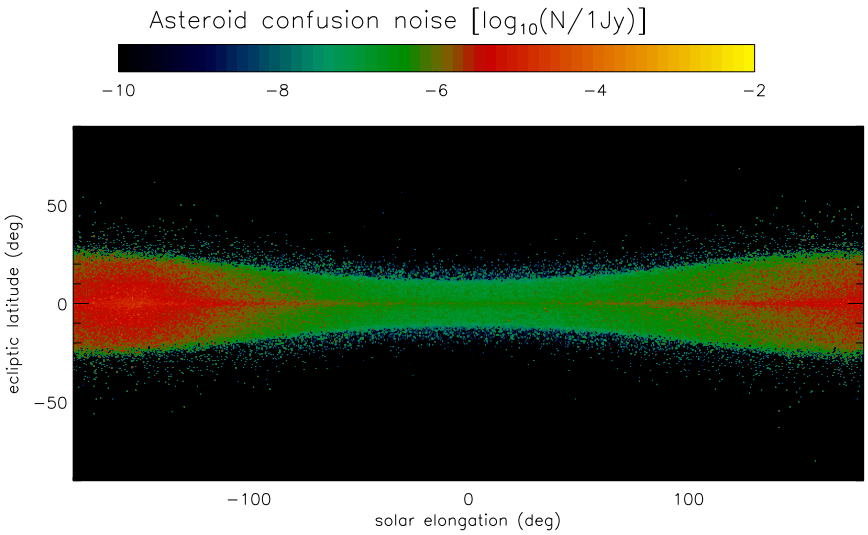

Figure 1: *Asteroid confusion noise (1σ per pixel) in the 18.3 μm (L18W) of the Akari/IRC instrument (former ASTRO-F). The Sun is located in the figure at (0,0) and the highest confusion noise can be seen in the anti-solar direction ($\lambda - \lambda_\odot = 180^\circ$). The asteroid component dominates the confusion noise in the ecliptic plane at solar elongations $|\lambda - \lambda_\odot| \geq 30^\circ$. Akari observations take place at $|\lambda - \lambda_\odot| = 90^\circ \pm 1^\circ$.*

few hundred Kelvin. With these temperatures, most of the heat is emitted at mid-IR wavelengths. Asteroids further out in the Solar System (e.g. in the Kuiper belt) have lower temperatures, therefore have their peak emission at far-IR wavelengths. However, due to geometry effects, the absolute flux drops quadratically with the distance from the observer. We demonstrate this effect in Fig. 2 where the spectral energy distribution of the same asteroid is plotted, if placed at different Earth/Sun distances in the Solar System.

The observed far-IR flux at longer wavelengths is decreasing rapidly despite the fact that the emission peaks shift to longer wavelengths as the target moves further from the Sun. E.g. at 70 μm 100 asteroids at 2 AU would produce roughly the same confusion contribution as 10^{10} (!) asteroids of similar size at 50 AU. Therefore an enormous population of relatively large bodies would be needed to have an effect comparable to that of main belt asteroids on the far-infrared confusion noise and expected counts of asteroids.

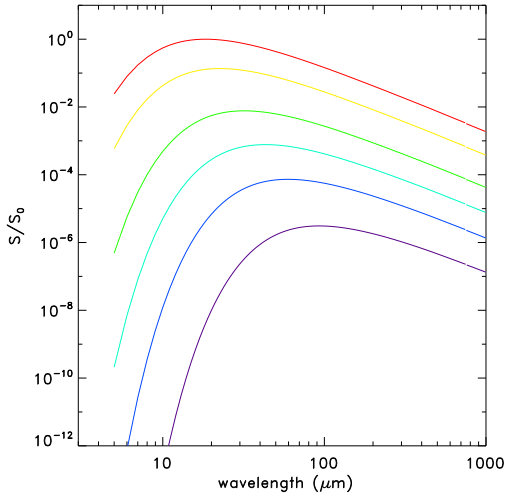

Figure 2: *Demonstration of the effect of the increasing Earth/Sun distance on the observed fluxes of the asteroids. S/S_0 is the ratio of measured S flux value at a specific wavelength and the reference flux value S_0 (the maximum value of the spectral energy distribution at $\Delta = 1\,AU$). The curves correspond to $\Delta = 1$, 2, 5, 10, 20 and 50 AU, from top to bottom, respectively and $r_\odot = \Delta + 1\,AU$ in all cases.*

Acknowledgement

This research was supported by the European Space Agency (ESA) via the PECS programme (#98011), and is part of the on-ground preparatory phase of the Herschel mission. We appreciate the support of the Hungarian Research Fund (OTKA, grant no. K62304) as well.

References

Harris, A. W. 1998, Icarus 131, 291

Jeong, W.S., Lee, H.M., Pak, S., et al., 2005, MNRAS, 357, 535

Jeong, W.S., Pearson, C.P., Lee, H.M., Pak, S., Nakagawa, T., 2006, MNRAS, in press [astro-ph/0603163]

Kiss, Cs., Klaas, U., Lemke, D., 2005, A&A 430, 343

Lebofsky, L. A., Sykes, M. V., Tedesco, E. F. et al. 1986, Icarus 68, 239

Meadows, V.S., Bhattacharya, B., Reach, W.T. et al., 2004, ApJS 154, 469

Müller, T. G., Blommaert, J. A. D. L. 2004, A&A 418, 347

Negrello, M., Magliocchetti, M., Moscardini, L., 2004, MNRAS 352, 493

Tedesco, E.F., Désert, F.-X., 2002, AJ 123, 2070

Tedesco, E.F., Cellino, A.; Zappalá, V., 2005, AJ 129, 2869